Impact of nonzero boresight pointing error on ergodic capacity of MIMO FSO communication systems

Rubén Boluda-Ruiz,[1,*] **Antonio García-Zambrana,**[1] **Beatriz Castillo-Vázquez,**[1] **and Carmen Castillo-Vázquez**[2]

[1]*Department of Communications Engineering, University of Málaga, E-29071 Málaga, Spain*
[2]*Department of Mathematical Analysis, Statistics and Operations Research and Applied Mathematics, University of Málaga, E-29071 Málaga, Spain*
[*]*rbr@ic.uma.es*

Abstract: A thorough investigation of the impact of nonzero boresight pointing errors on the ergodic capacity of multiple-input/multiple-output (MIMO) free-space optical (FSO) systems with equal gain combining (EGC) reception under different turbulence models, which are modeled as statistically independent, but not necessarily identically distributed (i.n.i.d.) is addressed in this paper. Novel closed-form asymptotic expressions at high signal-to-noise ratio (SNR) for the ergodic capacity of MIMO FSO systems are derived when different geometric arrangements of the receive apertures at the receiver are considered in order to reduce the effect of nonzero inherent boresight displacement, which is inevitably present when more than one receive aperture is considered. As a result, the asymptotic ergodic capacity of MIMO FSO systems is evaluated over log-normal (LN), gamma-gamma (GG) and exponentiated Weibull (EW) atmospheric turbulence in order to study different turbulence conditions, different sizes of receive apertures as well as different aperture averaging conditions. It is concluded that the use of single-input/multiple-output (SIMO) and MIMO techniques can significantly increase the ergodic capacity respect to the direct path link when the inherent boresight displacement takes small values, i.e. when the spacing among receive apertures is not too big. The effect of nonzero additional boresight errors, which is due to the thermal expansion of the building, is evaluated in multiple-input/single-output (MISO) and single-input/single-output (SISO) FSO systems. Simulation results are further included to confirm the analytical results.

© 2016 Optical Society of America

OCIS codes: (010.1330) Atmospheric turbulence; (060.2605) Free-space optical communication; (060.4510) Optical communications.

References and links

1. M. A. Khalighi and M. Uysal, "Survey on free space optical communication: A communication theory perspective," IEEE Communications Surveys Tutorials **16**(4), 2231–2258 (2014).
2. L. Andrews, R. Phillips, and C. Hopen, *Laser Beam Scintillation with Applications*, vol. 99 (SPIE, 2001).
3. F. Yang, J. Cheng, T. Tsiftsis, "Free-space optical communication with nonzero boresight pointing errors," IEEE Trans. Commun. **62**(2), 713–725 (2014).
4. J.-Y. Wang, J.-B. Wang, M. Chen, Y. Tang, and Y. Zhang, "Outage analysis for relay-aided free-space optical communications over turbulence channels with nonzero boresight pointing errors," IEEE Photonics J. **6**(4), 1–15 (2014).

#255615 Received 11 Dec 2015; revised 22 Jan 2016; accepted 28 Jan 2016; published 10 Feb 2016
© 2016 OSA

5. X. Yi and M. Yao, "Free-space communications over exponentiated Weibull turbulence channels with nonzero boresight pointing errors," Opt. Express **23**(3), 2904–2917 (2015).
6. I. Ansari, M.-S. Alouini, and J. Cheng, "Ergodic capacity analysis of free-space optical links with nonzero boresight pointing errors," IEEE Trans. Wireless Commun. **14**(8), 4248–4264 (2015).
7. L. C. Andrews and R. L. Phillips, *Laser Beam Propagation through Random Media*, vol. 1, (SPIE, 2005).
8. M. A. Al-Habash, L. C. Andrews, and R. L. Phillips, "Mathematical model for the irradiance probability density function of a laser beam propagating through turbulent media," Opt. Eng. **40**, 8 (2001).
9. R. Barrios and F. Dios, "Exponentiated Weibull distribution family under aperture averaging for Gaussian beam waves," Opt. Express **20**(12), 13055–13064 (2012).
10. R. Barrios and F. Dios, "Exponentiated Weibull model for the irradiance probability density function of a laser beam propagating through atmospheric turbulence," Optics Laser Technol. **45**, 13–20 (2013).
11. X. Yi, Z. Liu, and P. Yue, "Average BER of free-space optical systems in turbulent atmosphere with exponentiated Weibull distribution," Opt. Lett. **37**(24), 5142–5144 (2012).
12. P. Wang, L. Zhang, L. Guo, F. Huang, T. Shang, R. Wang, and Y. Yang, "Average BER of subcarrier intensity modulated free space optical systems over the exponentiated Weibull fading channels," Opt. Express **22**(17), 20828–20841 (2014).
13. P. Wang, J. Qin, L. Guo, and Y. Yang, "BER Performance of FSO Limited by Shot and Thermal Noise over Exponentiated Weibull Fading Channels," to be accepted in "IEEE Photonics Technol. Lett." (2015).
14. M. Cheng, Y. Zhang, J. Gao, F. Wang, and F. Zhao, "Average capacity for optical wireless communication systems over exponentiated Weibull distribution non-Kolmogorov turbulent channels," Appl. Opt. **53**(18), 4011–4017 (2014).
15. P. Wang, T. Cao, L. Guo, R. Wang, and Y. Yang, "Performance Analysis of Multihop Parallel Free-Space Optical Systems Over Exponentiated Weibull Fading Channels," IEEE Photonics J. **7**(1), 1–17 (2015).
16. P. Sharma, A. Bansal, P. Garg, T. Tsiftsis, and R. Barrios, "Performance of FSO links under exponentiated Weibull turbulence fading with misalignment errors," in *2015 IEEE International Conference on Communications (ICC)* (IEEE, 2015), pp. 5110–5114.
17. P. Wang, J. Zhang, L. Guo, T. Shang, T. Cao, R. Wang, and Y. Yang, "Performance analysis for relay-aided multihop BPPM FSO communication system over exponentiated Weibull fading channels with pointing error impairments," IEEE Photonics J. **7**(4), 1–20 (2015).
18. E. J. Lee and V. W. S. Chan, "Part 1: optical communication over the clear turbulent atmospheric channel using diversity," IEEE J. Sel. Areas Commun. **22**(9), 1896–1906 (2004).
19. E. Bayaki, R. Schober, and R. K. Mallik, "Performance analysis of MIMO free-space optical systems in gamma-gamma fading," IEEE Trans. Commun. **57**(11), 3415–3424 (2009).
20. T. A. Tsiftsis, H. G. Sandalidis, G. K. Karagiannidis, and M. Uysal, "Optical wireless links with spatial diversity over strong atmospheric turbulence channels," IEEE Trans. Wireless Commun. **8**(2), 951–957 (2009).
21. C. Abou-Rjeily, "On the optimality of the selection transmit diversity for MIMO-FSO links with feedback," IEEE Commun. Lett. **15**(6), 641–643 (2011).
22. M. Bhatnagar, "Differential Decoding of SIM DPSK over FSO MIMO Links," IEEE Commun. Lett. **17**(1), 79–82 (2013).
23. P. Kaur, V. Jain, and S. Kar, "Performance analysis of free space optical links using multi-input multi-output and aperture averaging in presence of turbulence and various weather conditions," IET Commun. **9**(8), 1104–1109 (2015).
24. M. Kashani, M. Uysal, and M. Kavehrad, "On the performance of MIMO FSO communications over Double Generalized Gamma fading channels," in *2015 IEEE International Conference on Communications (ICC)*(IEEE, 2015), pp. 5144–5149.
25. S. Jiang, G. Yang, Y. Wei, M. Bi, Y. Lu, X. Zhou, M. Hu, and Q. Li, "Performance analysis of space-diversity free-space optical links over exponentiated Weibull channels," IEEE Photonics Technol. Lett. **27**(21), 2250–2252 (2015).
26. A. García-Zambrana, C. Castillo-Vázquez, and B. Castillo-Vázquez, "Outage performance of MIMO FSO links over strong turbulence and misalignment fading channels," Opt. Express **19**(14), 13480–13496 (2011).
27. A. García-Zambrana, B. Castillo-Vázquez, and C. Castillo-Vázquez, "Asymptotic error-rate analysis of FSO links using transmit laser selection over gamma-gamma atmospheric turbulence channels with pointing errors," Opt. Express **20**(3), 2096–2109 (2012).
28. A. Farid and S. Hranilovic, "Diversity gain and outage probability for MIMO free-space optical links with misalignment," IEEE Trans. Commun. **60**(2), 479–487 (2012).
29. L. Yang, M. O. Hasna, and X. Gao, "Asymptotic BER analysis of FSO with multiple receive apertures over $\mathscr{M}$-distributed turbulence channels with pointing errors," Opt. Express **22**(15), 18238–18245 (2014).
30. A. García-Zambrana, R. Boluda-Ruiz, C. Castillo-Vázquez, and B. Castillo-Vázquez, "Transmit alternate laser selection with time diversity for FSO communications," Opt. Express **22**(20), 23861–23874 (2014).
31. A. García-Zambrana, R. Boluda-Ruiz, C. Castillo-Vázquez, and B. Castillo-Vázquez, "Novel space-time trellis codes for free-space optical communications using transmit laser selection," Opt. Express **23**(19), 24195–24211 (2015).

#255615 Received 11 Dec 2015; revised 22 Jan 2016; accepted 28 Jan 2016; published 10 Feb 2016
© 2016 OSA

32. M. Bhatnagar and Z. Ghassemlooy, "Performance evaluation of FSO MIMO links in Gamma-Gamma fading with pointing errors," in *2015 IEEE International Conference on Communications (ICC)*(IEEE, 2015), pp. 5084–5090.
33. D. A. Luong, T. C. Thang, and A. T. Pham, "Average capacity of MIMO/FSO systems with equal gain combining over log-normal channels," in *2013 Fifth International Conference on Ubiquitous and Future Networks (ICUFN)*(IEEE, 2013), pp. 306–309.
34. P. Deng, M. Kavehrad, Z. Liu, Z. Zhou, and X. Yuan, "Capacity of MIMO free space optical communications using multiple partially coherent beams propagation through non-Kolmogorov strong turbulence," Opt. Express **21**(13), 15213–15229 (2013).
35. D. A. Luong and A. T. Pham, "Average capacity of MIMO free-space optical gamma-gamma fading channel," in *2014 IEEE International Conference on Communications (ICC)* (IEEE, 2014), pp. 3354–3358.
36. P. Kaur, V. K. Jain, and S. Kar, "Capacity of free space optical links with spatial diversity and aperture averaging," in *2014 27th Biennial Symposium on Communications (QBSC)*(IEEE, 2014), pp. 14–18.
37. J. Zhang, L. Dai, Y. Han, Y. Zhang, and Z. Wang, "On the ergodic capacity of MIMO free-space optical systems over turbulence channels," IEEE J. Sel. Areas Commun. **33**(9), 1925–1934 (2015).
38. R. Boluda-Ruiz, A. García-Zambrana, B. Castillo-Vázquez, and C. Castillo-Vázquez, "On the capacity of MISO FSO systems over gamma-gamma and misalignment fading channels," Opt. Express **23**(17), 22371–22385 (2015).
39. J. A. Anguita, M. A. Neifeld, and B. V. Vasic, "Spatial correlation and irradiance statistics in a multiple-beam terrestrial free-space optical communication link," Appl. Opt. **46**(26), 6561–6571 (2007).
40. J. A. Anguita and J. E. Cisternas, "Experimental evaluation of transmitter and receiver diversity in a terrestrial FSO link," in *2010 IEEE GLOBECOM Workshops (GC Wkshps),*(IEEE, 2010), pp. 1005–1009.
41. I. I. Kim, B. McArthur, and E. J. Korevaar, "Comparison of laser beam propagation at 785 nm and 1550 nm in fog and haze for optical wireless communications," in *Information Technologies 2000*(ISOP, 2001), pp. 26–37.
42. A. K. Majumdar and J. C. Ricklin, *Free-Space Laser Communications: Principles and Advances*, vol. 2 (Springer Science and Business Media, 2010).
43. I. S. Gradshteyn and I. M. Ryzhik, *Table of Integrals, Series and Products*, 7th ed. (Academic Inc., 2007).
44. N. Wang and J. Cheng, "Moment-based estimation for the shape parameters of the gamma-gamma atmospheric turbulence model," Opt. Express **18**(12), 12824–12831 (2010).
45. F. S. Vetelino, C. Young, L. Andrews, and J. Recolons, "Aperture averaging effects on the probability density of irradiance fluctuations in moderate-to-strong turbulence," Appl. Opt. **46**(11), 2099–2108 (2007).
46. S. D. Lyke, D. G. Voelz, and M. C. Roggemann, "Probability density of aperture-averaged irradiance fluctuations for long range free space optical communication links," Appl. Opt. **48**(33), 6511–6527 (2009).
47. L. C. Andrews, R. L. Phillips, C. Y. Hopen, and M. A. Al-Habash, "Theory of optical scintillation," J. Opt. Soc. Am. A **16**(6), 1417–1429 (1999).
48. L. C. Andrews, R. L. Phillips, and C. Y. Hopen, "Aperture averaging of optical scintillations: power fluctuations and the temporal spectrum," Waves Random Media **10**(1), 53–70 (2000).
49. A. A. Farid and S. Hranilovic, "Outage capacity optimization for free-space optical links with pointing errors," J. Lightwave Technol. **25**(7), 1702–1710 (2007).
50. S. Arnon, "Effects of atmospheric turbulence and building sway on optical wireless-communication systems," Opt. Lett. **28**(2), 129–131 (2003).
51. D. K. Borah and D. G. Voelz, "Pointing error effects on free-space optical communication links in the presence of atmospheric turbulence," J. Lightwave Technol. **27**(18), 3965–3973 (2009).
52. A. Lapidoth, S. Moser, and M. Wigger, "On the Capacity of Free-Space Optical Intensity Channels," IEEE Trans. Inf. Theory **55**(10), 4449–4461 (2009).
53. R. Boluda-Ruiz, A. García-Zambrana, B. Castillo-Vázquez, and C. Castillo-Vázquez, "Ergodic capacity analysis for DF strategies in cooperative FSO systems," Opt. Express **23**(17), 21565–21584 (2015).
54. F. Yilmaz and M.-S. Alouini, "Novel asymptotic results on the high-order statistics of the channel capacity over generalized fading channels," in *2012 IEEE 13th International Workshop on Signal Processing Advances in Wireless Communications (SPAWC)*(IEEE, 2012), pp. 389–393.
55. I. Ansari, F. Yilmaz, and M. Alouini, "Performance Analysis of Free-Space Optical Links Over Malaga ($\mathscr{M}$) Turbulence channels with pointing errors," IEEE Trans. Wireless Commun. **15**(1), 91–102 (2016).
56. R. Boluda-Ruiz, A. Garcia-Zambrana, B. Castillo-Vazquez, and C. Castillo-Vazquez, "Ergodic capacity analysis of decode-and-forward relay-assisted FSO systems over alpha-mu fading channels considering pointing errors," IEEE Photonics J. **8**(1), 1–11 (2016).
57. Wolfram Research, Inc., "The Wolfram functions site," URL http://functions.wolfram.com.
58. A. Jurado-Navas, J. M. Garrido-Balsells, J. F. Paris, and A. Puerta-Notario, "A Unifying Statistical Model for Atmospheric Optical Scintillation," in *Numerical Simulations of Physical and Engineering Processes*, Dr. J. Awrejcewicz ed. (Intech, 2011).
59. M. Kashani, M. Uysal, and M. Kavehrad, "A novel statistical model for turbulence-induced fading in free-space optical systems," in *2013 15th International Conference on Transparent Optical Networks (ICTON)*(IEEE, 2013), pp. 1–5.
60. M. Aminikashani, M. Uysal, and M. Kavehrad, "On the Performance of MIMO FSO Communications over

#255615 Received 11 Dec 2015; revised 22 Jan 2016; accepted 28 Jan 2016; published 10 Feb 2016
© 2016 OSA

Double Generalized Gamma Fading Channels," arXiv preprint arXiv:1502.00365 (2015).
61. S. Nadarajah and A. K. Gupta, "On the moments of the exponentiated Weibull distribution," Commun. Statistics-Theory Methods **34**(2), 253–256 (2005).

1. Introduction

Free-space optical (FSO) communication systems have attracted a considerable attention as an efficient solution due to their advantages including a huge license free spectrum, immunity to interference as well as an excellent security. In comparison to radio-frequency (RF) systems, the FSO systems have quite a high optical bandwidth available, allowing high-speed data transmission. The most important applications for which the FSO systems are used include metropolitan area network (MAN) extension and local area network (LAN)-to-LAN connectivity among others [1]. Despite the advantages of FSO technology, such systems are not without disadvantages. Atmospheric turbulence and pointing errors are the most damaging phenomena in FSO systems. Atmospheric turbulence results in fluctuations in both the intensity and the phase of the received signal, severely degrading the link performance [2]. In addition to this, pointing errors can also deteriorate the performance of FSO systems. Thermal expansions, dynamic wind loads and weak earthquakes result in the building sway that causes mechanical vibration of the transmitter beam leading to a misalignment between transmitter and receiver. The effect of pointing error consists of three essential parameters: beam width, jitter and boresight displacement. The beam width represents the beam waist (radius computed at e^{-2}), the jitter represents the random offset of the beam center at receive aperture plane and the boresight represents the fixed displacement between beam center and the alignment point. It should, however, be noted that there are two kinds of boresight displacements: the inherent boresight displacement and the additional boresight error. The first of them is related to the spacing among receive apertures at the receiver. This inherent boresight displacement represents a fixed distance, i.e., the distance between each receive aperture and the corresponding alignment point. The second one is related to the boresight error that is due to the thermal expansion of the building, which was defined in [3]. Although a FSO communication system can be installed with an additional boresight error close to zero or even negligible, the inherent boresight displacement must necessarily always be taken into account at the receiver when more than one receive aperture is assumed in order to increase the performance by using receive-diversity. The latter is due to the fact that each laser can be aligned with only one receive aperture and, hence, there is an inherent boresight displacement that depends on the spacing among receive apertures, the corresponding alignment point as well as the geometric arrangement of the receive apertures. To the best of authors' knowledge, there are not many research articles that take into consideration the effect of nonzero boresight pointing errors on the performance of FSO communication systems when only one receive aperture is considered [4–6], but there are none when more than one receive aperture is assumed. In [4] the outage probability for both the parallel and serial relay-assisted FSO communications is analyzed over $\mathscr{M}$-distributed atmospheric turbulence with nonzero boresight pointing errors. In [5] the performance of FSO links in terms of the bit error-rate (BER) and outage probability is studied over exponentiated Weibull fading channels with nonzero boresight pointing errors. In [6] the asymptotic ergodic capacity of FSO links is evaluated over atmospheric turbulence fading channels with nonzero boresight pointing errors. A unified approach for computing the moments of a single FSO link was presented for different statistical models of atmospheric turbulence.

Different statistical models have been proposed for modeling the atmospheric turbulence in the literature. The most widely accepted model under weak turbulence conditions is the log-normal (LN) model, which was obtained a few years ago in [7]. Another atmospheric turbulence model is the gamma-gamma (GG) distribution, which has gained a wide acceptance for

#255615 Received 11 Dec 2015; revised 22 Jan 2016; accepted 28 Jan 2016; published 10 Feb 2016
© 2016 OSA

moderate-to-strong turbulence regime [7, 8]. Recently, a new atmospheric turbulence model, called exponentiated Weibull (EW), has been proposed in [9, 10]. In [9] was shown that EW distribution offers an excellent fit to simulation and experimental data under weak aperture averaging conditions. However, the EW parameters obtained in [9, eqs. (10)-(12)] do not have the expected accuracy for the point-like receive apertures. In [10], was also demonstrated that EW distribution offers an excellent fit to simulation and experimental data under moderate-to-strong aperture averaging conditions using other equations [10, eqs. (20)-(22)]. The EW distribution has been used in a significant number of research articles [11–13] in order to study the performance of FSO communication systems. The combined effect of EW atmospheric turbulence and pointing errors has been studied in [5, 14–17]. In addition to this, expressions obtained in [10, eqs. (20)-(22)] for the EW parameters were used in [14] in order to study the ergodic capacity.

For many years researchers have proved that a much higher performance of FSO systems in terms of the BER and outage probability is achieved when fading-mitigation techniques are used such as creating spatial diversity based on multiple-input/multiple-output (MIMO) FSO system with multiple lasers at the transmitter and/or multiple receive apertures at the receiver. In the last decade, the effect of the atmospheric turbulence on MIMO FSO systems without considering pointing errors has been studied in [18–20]. But even at this time, there are a few research articles that have studied MIMO FSO systems over atmospheric turbulence without considering pointing errors such as [21–25]. The combined effect of atmosphere and misalignment fading with zero boresight error has been analyzed in terms of the BER and outage probability in the case of multiple-input/single-output (MISO), SIMO as well as MIMO FSO channels in [26–32]. Newly, the study of ergodic capacity for FSO channels has generated a recent motivation in the community research. In FSO communications, MIMO systems can be employed to reduce scintillation and therefore improves FSO channel capacity. However, to our knowledge, only a few works have studied the ergodic capacity of MIMO FSO systems but not considering the effect of pointing errors, only taking into account the effect of the atmospheric turbulence [33–37]. Nevertheless, the effect of pointing errors was taken into account in [38], where a closed-form expression for the ergodic capacity was derived in terms of the H-Fox function, demonstrating that the effect of zero boresight pointing errors only depends on the number of lasers and pointing error parameters on MISO FSO communication systems.

In the present study we perform a thorough investigation of the impact of nonzero boresight pointing errors on the ergodic capacity of MIMO FSO systems with equal gain combining (EGC) reception under different turbulence models, which are modeled as statistically independent, but not necessarily identically distributed (i.n.i.d.). To our knowledge, there is neither a closed-form expression nor an asymptotic expression for the ergodic capacity of MIMO FSO communication systems over atmospheric turbulence with nonzero boresight pointing errors. In this way, novel closed-form asymptotic expressions at high signal-to-noise ratio (SNR) for the ergodic capacity of MIMO FSO systems are derived when different geometric arrangements of the receive apertures at the receiver is considered in order to reduce the effect of nonzero inherent boresight displacement, which is inevitably present when more than one receive aperture is considered. For convenience, this asymptotic analysis is only studied at high SNR due to the fact that a greater capacity is required for potential FSO applications nowadays. As a result, the asymptotic ergodic capacity of MIMO FSO systems is evaluated over LN, GG as well as EW atmospheric turbulence in order to study different turbulence conditions, different sizes of receive apertures as well as different aperture averaging conditions. Additionally, a new methodology is proposed in order to generate different receiver configurations from the juxtaposition of equilateral triangles when all lasers are aligned with the centroid (p_c) of the formed geometric figure, which guarantee a notable reduction of the effect of the inherent boresight

#255615 Received 11 Dec 2015; revised 22 Jan 2016; accepted 28 Jan 2016; published 10 Feb 2016
© 2016 OSA

displacement against other geometric arrangements of the receive apertures.

2. System model

We adopt a MIMO FSO communication system with M transmitters or laser sources and N receive apertures. The use of infrared technologies based on intensity-modulation and direct-detection (IM/DD) is assumed here. IM/DD systems are commonly used in the terrestrial FSO links due to their simplicity and low cost. The intensity of the emitted light is used for transmitting the information. In other words, the input signal is proportional to the light intensity and is therefore non-negative. The photodetector directly detects changes in the light intensity without the need for a local oscillator. Here, the EGC reception technique is adopted due to its considerable lower implementation complexity even maintaining relevant performance in FSO links [19, 20].

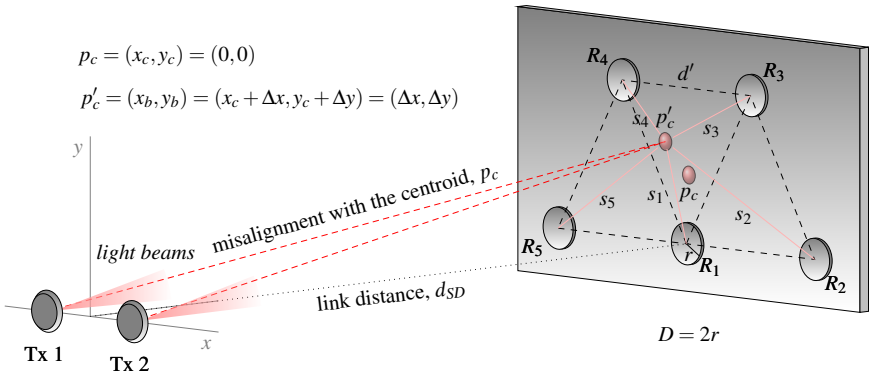

Fig. 1. Block diagram of the considered MIMO FSO communications system.

An example of a MIMO FSO system with $M = 2$ and $N = 5$ is depicted in Fig. 1 for a source-destination link distance of d_{SD}, where all lasers are aligned with the centroid (alignment point located in $p_c = (x_c, y_c) = (0,0)$) of the geometric arrangement of the receive apertures, which is a trapeze. The latter statement will be explained in more detail in the subsection 2.1. It must be noted that all receive apertures are separated by a fixed distance equals d' (as shown in Fig. 1 in black dashed line) in order to consider uncorrelated fading, which depends on the coherence length of the atmospheric turbulence, l_c. On the one hand, note that the minimum value of the spacing among receive apertures is equal to $d' = l_c$ in order to assume uncorrelated fading as long as this spacing is technically feasible for potential FSO applications. On the other hand, a greater spacing among receive apertures leads to an increase in the inherent boresight displacement at the receiver plane. Additionally, the laser sources are separated by a fixed distance so that uncorrelated fading can also be considered at the transmitter [38–40]. Before evaluating the corresponding expression of the total boresight displacement, i.e. taking into account both the inherent boresight displacement and the additional boresight error, we firstly obtain the expression of the inherent boresight displacement assuming that the additional boresight error is set to zero. In other words, assuming that $p_c = p'_c$. In this case, the inherent boresight displacement is equal to the Euclidean distance between each receive aperture and the corresponding alignment point, i.e. the centroid p_c, which is defined as $d_{R_k - p_c}$ for $k = 1 \ldots N$. Hence, the boresight displacement is given by $s_k = d_{R_k - p_c}$. In order to add the additional boresight error to this analysis, we have to rewrite the expression of s_k but considering a nonzero additional boresight error. When there is a nonzero additional boresight error, the alignment point becomes p'_c instead of p_c. Hence, knowing that $p'_c = (x_c + \Delta x, y_c + \Delta y) = (\Delta x, \Delta y)$, it can easily be deduced

#255615 Received 11 Dec 2015; revised 22 Jan 2016; accepted 28 Jan 2016; published 10 Feb 2016
© 2016 OSA

that the expression corresponding to the total boresight displacement of each receiver aperture when all lasers are aligned with the centroid is given by

$$s_k = \sqrt{d^2_{R_k - p_c} + \Delta x^2 + \Delta y^2 - 2\left(\Delta x \cdot x_k + \Delta y \cdot y_k\right)}, \qquad k = 1 \ldots N \tag{1}$$

where (x_k, y_k) represents the receive aperture location corresponding to R_k for $k = 1 \ldots N$. The additional boresight error (s_{AB}) is given by the Euclidean distance between p_c and p'_c, i.e. $s_{AB} = \sqrt{\Delta x^2 + \Delta y^2}$.

2.1. Analysis of the proposed geometric arrangement for the receiver

With the goal of reducing the effect of the inherent boresight displacement, we propose an interesting solution for the geometric arrangement at the receiver, as shown in Fig. 2, from the juxtaposition of equilateral triangles and considering the centroid of each figure as an alignment point in order to balance the distance between the alignment point and each receive aperture. Firstly, we start with the easiest case, i.e. the case of two receive apertures, which are separated

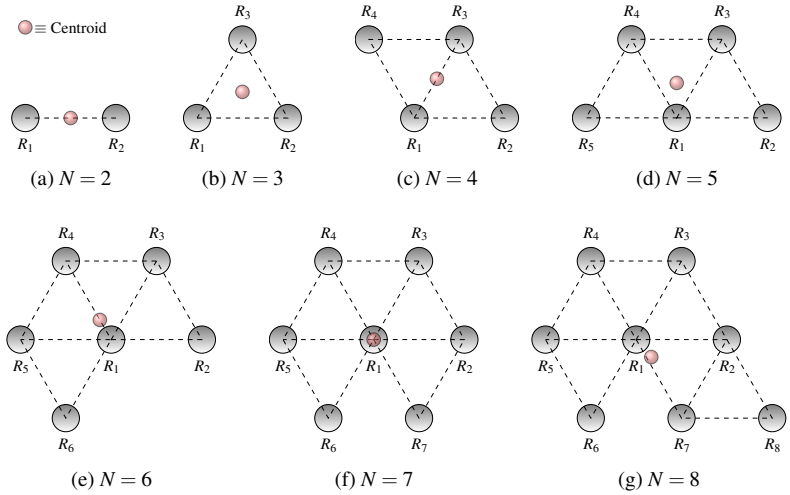

Fig. 2. Different geometric arrangement for the receiver from the juxtaposition of equilateral triangles.

by a distance equals d', as shown in Fig. 2(a). Note that the distance d' should sufficiently be larger than the coherence length in order to assume uncorrelated fading. In order to add one more receive aperture to the geometric arrangement, the next formed figure should be a equilateral triangle, where all receive apertures are at the same distance, as shown in Fig. 2(b), and, hence, the inherent boresight displacement is reduced. The following formed figure is a diamond, as shown in Fig. 2(c), which is generated from the juxtaposition of two equilateral triangles. It is noteworthy to mention that the total area formed by all receive apertures is also reduced. And the next one is a trapeze, as shown in Fig. 2(d), when there are five receive apertures at the receiver. This method consists of adding receive apertures to the receiver always around the centroid of the formed geometric arrangement, and so on.

3. Channel model

The received electrical signal for a FSO link is given by $Y = \eta XI + Z$, where η is the detector responsivity, assumed hereinafter to be the unity, X represents the optical power supplied by the source, I is the equivalent real-value fading gain (irradiance) through the channel between

#255615 Received 11 Dec 2015; revised 22 Jan 2016; accepted 28 Jan 2016; published 10 Feb 2016
© 2016 OSA

the source and the receiver, and Z is additive white Gaussian noise (AWGN) with zero mean and variance $\sigma^2 = N_0/2$, i.e. $Z \sim N(0, N_0/2)$, independent of the on/off state of the received bit. The irradiance is considered to be a product of three factors, i.e. $I = L \cdot I^a \cdot I^p$, atmospheric path loss L, atmospheric turbulence I^a, and geometric spread and pointing errors I^p. L is determined by the exponential Beers-Lambert law as $L = e^{-\Phi d_{SD}}$, where d_{SD} is the link distance and Φ is the atmospheric attenuation coefficient. It is given by $\Phi = (3.91/V(km))\,(\lambda(nm)/550)^{-q}$ where V is the visibility in kilometers, λ is the wavelength in nanometers and q is the size distribution of the scattering particles, being $q = 1.3$ for average visibility (6 km $< V <$ 50 km), and $q = 0.16V + 0.34$ for haze visibility (1 km $< V <$ 6 km) [41]. Next, we examine some atmospheric turbulence models as well as the nonzero boresight pointing error model.

3.1. Atmospheric turbulence models

In order to study the effects of nonzero boresight pointing errors on the ergodic capacity of MIMO FSO communication systems, several statistical models for characterizing the atmospheric turbulence have been considered here. As commented before, atmospheric turbulence causes fluctuations in both the intensity and the phase of the received signal due to variations in the refractive index along the FSO link. In this way, the LN turbulence model is the most widely accepted model under weak turbulence conditions, which was proposed several decades ago in [7]. The PDF corresponding to LN model is given by

$$f_{I^a}^{LN}(i) = \frac{1}{i\sqrt{8\pi\sigma_X^2}} \exp\left(-\frac{\left(\ln(i) + 2\sigma_X^2\right)^2}{8\sigma_X^2}\right), \quad i \geq 0 \tag{2}$$

where σ_X^2 is the log-amplitude variance given by $\sigma_X^2 \approx \sigma_R^2/4$. The parameter $\sigma_R^2 = 1.23\kappa^{7/6} C_n^2 d_{SD}^{11/6}$ represents the Rytov variance for a plane wave, which is a measure of optical turbulence strength. Here, $\kappa = 2\pi/\lambda$ is the optical wave number, λ is the wavelength and d_{SD} is the link distance in meters. C_n^2 is the refractive index structure parameter, which is the most significant parameter that determines the turbulence strength. Clearly, C_n^2 not only depends on the altitude, but also on the local conditions such as terrain type, geographic location, cloud cover, and time of day [42]. In addition, C_n^2 is typically in the range 10^{-13}-to-10^{-17} $m^{-2/3}$ [2]. It is well known that the LN turbulence model is not appropriate for moderate-to-strong turbulence conditions. For that reason, the GG turbulence model is also assumed in order to consider a wide range of turbulence conditions, i.e. moderate-to-strong, [2, 8], whose PDF is given by

$$f_{I^a}^{GG}(i) = \frac{2(\alpha\beta)^{(\alpha+\beta)/2}}{\Gamma(\alpha)\Gamma(\beta)} i^{((\alpha+\beta)/2)-1} K_{\alpha-\beta}\left(2\sqrt{\alpha\beta i}\right), \quad i \geq 0 \tag{3}$$

where the parameters α and β represent the effective numbers of large- and small-scale turbulence cells, and $\Gamma(\cdot)$ is the well-known Gamma function and $K_\nu(\cdot)$ is the νth-order modified Bessel function of the second kind [43, eqn. (8.43)]. The parameters α and β can be selected to achieve a good agreement between Eq. (3) and measurement data [8]. Alternatively, assuming negligible inner scale and plane wave propagation, α and β can directly be linked to physical parameters through the following expresions [8, 44]:

$$\alpha = \left[\exp\left(0.49\sigma_R^2/(1 + 1.11\sigma_R^{12/5})^{7/6}\right) - 1\right]^{-1}, \tag{4a}$$

$$\beta = \left[\exp\left(0.51\sigma_R^2/(1 + 0.69\sigma_R^{12/5})^{5/6}\right) - 1\right]^{-1}. \tag{4b}$$

#255615 Received 11 Dec 2015; revised 22 Jan 2016; accepted 28 Jan 2016; published 10 Feb 2016
© 2016 OSA

It must be emphasized that parameters α and β cannot arbitrarily be chosen in FSO applications, being related through the Rytov variance. In this fashion, it can be shown that the relationship $\alpha > \beta$ always holds, and the parameter β is lower bounded above 1 as the Rytov variance approaches ∞. It must be noted that the value of the Rytov variance can also be used for characterizing different turbulence levels: weak-turbulence refers to $\sigma_R^2 \leq 0.3$, moderate-turbulence has $0.3 < \sigma_R^2 \leq 5$ and strong-turbulence corresponds to $\sigma_R^2 > 5$ [44]. Additionally, a new turbulence model, i.e. EW, was recently proposed in [9] in order to consider a wide range of turbulence conditions (weak-to-strong) as well as aperture averaging conditions, since the GG turbulence model does not provide a good fit to simulation data in moderate-to-strong turbulence regimes when $D \geq \rho_0$ [45, 46]. D represents the diameter of a circular detection aperture ($D = 2r$) and ρ_0 represents the plane wave coherence radius [47]. At this point, it is noteworthy to mention that a fading reduction is achieved by aperture averaging, which can be quantified by considering the aperture averaging factor $A = \sigma_I^2(D)/\sigma_I^2(0)$, where $\sigma_I^2(D)$ and $\sigma_I^2(0)$ denote the scintillation indexes for a receive aperture of diameter D and a point-like receiver, respectively [7]. It should be highlighted that the aperture averaging has been analyzed by some authors, obtaining much better results under moderate-to-strong turbulence conditions [48]. Furthermore, it was shown in [9, 10] that the EW distribution offers an excellent fit to simulation and experimental data under all aperture averaging conditions $D \geq \rho_0$, in weak-to-strong turbulence regimes. Hence, the EW distribution is considered in order to include the effects from the aperture averaging [9, eqn. (7)], whose PDF is given by

$$f_{I^a}^{EW}(i) = \frac{ab}{c}\left(\frac{i}{c}\right)^{b-1} \exp\left(-\left(\frac{i}{c}\right)^{b}\right)\left\{1-\exp\left(-\left(\frac{i}{c}\right)^{b}\right)\right\}^{a-1}, \quad i \geq 0 \tag{5}$$

where $b > 0$ is a shape parameter related to the scintillation index (SI), $c > 0$ is scale parameter related to the mean value of the irradiance and $a > 0$ is an extra shape parameter that is strongly dependent on the receiver aperture size. By fitting the EW turbulence model to some simulated or experimental PDF data, several specific values of the parameters a, b and c as well as some expressions for evaluating these parameters have been obtained in [9, 10]. In this study, expressions obtained in [10, eqs. (20)-(22)] are used for moderate-to-strong turbulence conditions, which are valid when the aperture averaging $A < 0.9$ [10]. The expressions corresponding to the EW parameters are given as a function of the scintillation index, σ_I^2, as follows

$$a = \frac{7.220\sigma_I^{2/3}}{\Gamma\left(2.487\sigma_I^{2/6}\right) - 0.104}, \quad b = 1.012(a\sigma_I^2)^{-13/25} + 0.142, \quad c = \frac{1}{a\Gamma(1+1/b)\, g_1(a,b)}, \tag{6}$$

where $g_n(a,b)$ is defined as follows

$$g_n(a,b) = \sum_{k=0}^{\infty} \frac{(-1)^k \Gamma(a)}{k!(k+1)^{1+n/b}\Gamma(a-k)}. \tag{7}$$

Knowing that the plane wave coherence radius ρ_0 is defined as $\rho_0 = 0.79\left(C_n^2\kappa^2 d_{SD}\right)^{-3/5}$ in both weak and strong turbulence conditions, the coherence length of irradiance fluctuations is determined by the Fresnel zone $\sqrt{d_{SD}/\kappa}$ under weak turbulence, whereas the coherence length of irradiance fluctuations is defined by the plane wave coherence radius ρ_0 under strong turbulence [38, 47].

3.2. Nonzero boresight pointing error model

Regarding the impact of pointing errors, we use a model of misalignment fading given in [49], which was extended in [3] to take into account the boresight displacement at the detector,

#255615 Received 11 Dec 2015; revised 22 Jan 2016; accepted 28 Jan 2016; published 10 Feb 2016
© 2016 OSA

wherein the effect of beam width, detector size and jitter variance is considered. Building sway can be caused by strong winds, thermal expansion of building frame parts, and weak earthquakes [50]. Although the effects of turbulence and pointing are not strictly independent, for smaller jitter values they can be approximated as independent [51]. Hence, both atmospheric turbulence and pointing errors can be considered to be statistically independent. Assuming a Gaussian spatial intensity profile of beam waist radius, ω_z, on the receiver plane at distance z from the transmitter and a circular receive aperture of radius r, the PDF of nonzero boresight pointing error, $f_{I^p}^{NZB}(i)$, was derived in [3] as

$$f_{I^p}^{NZB}(i) = \frac{\varphi^2 i^{\varphi^2-1}}{A_0^{\varphi^2}} \exp\left(-\frac{s^2}{2\sigma_s^2}\right) I_0\left(\frac{s}{\sigma_s}\sqrt{-2\varphi^2 \ln\left(\frac{i}{A_0}\right)}\right), \quad 0 \le i \le A_0 \tag{8}$$

where $\varphi = \omega_{z_{eq}}/2\sigma_s$ is the ratio between the equivalent beam radius at the receiver and the pointing error displacement standard deviation (jitter) σ_s at the receiver, $A_0 = [\mathrm{erf}(v)]^2$ is the fraction of the collected power at $r = 0$, $\omega_{z_{eq}}^2 = \omega_z^2 \sqrt{\pi}\mathrm{erf}(v)/2v\exp(-v^2)$, $v = \sqrt{\pi}r/\sqrt{2}\omega_z$, s is the boresight displacement, which was defined in section 2 taking into account both inherent boresight displacement and additional boresight error, and $I_0(\cdot)$ is the modified Bessel function of the first kind with order zero. Here, independent identical Gaussian distributions for the elevation and the horizontal displacement (sway) are considered, being σ_s^2 the jitter variance at the receiver. It should be noted that when zero boresight pointing errors is considered, i.e. $s = 0$, the PDF in Eq. (8) reduces to the pointing errors model proposed in [49] as follows

$$f_{I^p}^{ZB}(i) = \frac{\varphi^2}{A_0^{\varphi^2}} i^{\varphi^2-1}. \quad 0 \le i \le A_0 \tag{9}$$

4. Asymptotic ergodic capacity analysis of MIMO FSO systems

In this section, the ergodic capacity as a performance measure is evaluated for a MIMO FSO communication system over LN, GG and EW fading channels with nonzero boresight pointing errors. It must be mentioned that the ergodic capacity for FSO links based on IM/DD systems represents a lower bound as given in [52] by Lapidoth. When the EGC reception is used at the receiver, the statistical channel model can be written as

$$Y = \frac{X}{MN}\sum_{k=1}^{M}\sum_{l=1}^{N} I_{kl} + Z_{\mathrm{EGC}}, \quad X \in \{0, 2P_{\mathrm{opt}}\}, \quad Z_{\mathrm{EGC}} \sim N(0, N_0/2), \tag{10}$$

where I_{kl} represents the equivalent irradiance through the optical channel between the kth transmit aperture and the lth receive aperture and X is either 0 or $2P_{\mathrm{opt}}$ (P_{opt} is the average optical power). Here, the division by M in Eq. (10) is considered so as to maintain the average optical power in the air at a constant level of P_{opt}, being transmitted by each laser an average optical power P_{opt}/M. In this way, the total transmit power is the same as in a FSO system with no transmit diversity, i.e. direct path link. Furthermore, the division by N is considered to ensure that the area of the receive aperture in single-input/single-output (SISO) FSO links has the same size as in the sum of N receive aperture areas [18]. The resulting received electrical SNR, γ_{MIMO}, can be defined as

$$\gamma_{\mathrm{MIMO}} = \frac{1}{2}\frac{\left(2P_{\mathrm{opt}}/MN\right)^2}{N_0/2}\left(\sum_{k=1}^{M}\sum_{l=1}^{N} I_{kl}\right)^2 = \frac{4\gamma_0}{M^2N^2}\left(\sum_{k=1}^{M}\sum_{l=1}^{N} I_{kl}\right)^2, \tag{11}$$

where $\gamma_0 = P_{\mathrm{opt}}^2/N_0$ represents the received electrical SNR in absence of turbulence. Assuming instantaneous channel side information at the receiver (CSIR), the ergodic capacity corresponding to the considered MIMO FSO system in bits/s/Hz is defined as

#255615 Received 11 Dec 2015; revised 22 Jan 2016; accepted 28 Jan 2016; published 10 Feb 2016
© 2016 OSA

$C_{\mathrm{MIMO}} = (B/2\ln(2))\mathbb{E}[\ln(1+\gamma_{\mathrm{MIMO}})]$, with $\mathbb{E}[\cdot]$ denoting expectation. Hence, this ergodic capacity, C_{MIMO}, can be obtained as follows

$$C_{\mathrm{MIMO}} = \frac{B}{2\ln(2)} \underbrace{\int_0^{\infty} \cdots \int_0^{\infty}}_{\text{MN-fold}} \ln\left(1 + \frac{4\gamma_0}{M^2N^2}\left(\sum_{k=1}^{M}\sum_{l=1}^{N} i_{kl}\right)^2\right) \prod_{k=1}^{M}\prod_{l=1}^{N} f_{I_{kl}}(i_{kl})di_{kl}, \tag{12}$$

where B is the channel bandwidth, $\ln(\cdot)$ is the natural logarithm [43, eqn. (1.511)] and, $f_{I_{kl}}(i_{kl})$ represents the combined PDF corresponding to the equivalent irradiance through the optical channel between the kth transmit aperture and the lth receive aperture. It should be noted that the factor $1/2$ in Eq. (12) is because the transmitter is assumed to operate in half-duplex mode. It must also be noted that deriving the PDF of $I_T = \sum_{k=1}^{M}\sum_{l=1}^{N} I_{kl}$ is tedious, if not impossible, and not readily tractable due to the difficulty in finding its statistics. Hence, a lower bound for this sum can be obtained by using the well-known inequality between arithmetic mean (AM) and geometric mean (GM) given by $AM \geq GM$, where $AM = (1/MN)\sum_{k=1}^{M}\sum_{l=1}^{N} I_{kl}$ and $GM = \sqrt[MN]{\prod_{k=1}^{M}\prod_{l=1}^{N} I_{kl}}$ are the arithmetic and geometric means, respectively. Therefore, a lower bound for the sum of $M \cdot N$ random variates can be obtained as

$$\sum_{k=1}^{M}\sum_{l=1}^{N} I_{kl} \geq MN \sqrt[MN]{F \cdot \prod_{k=1}^{M}\prod_{l=1}^{N} I_{kl}}. \tag{13}$$

From Eq. (13), it can easily be deduced that the mathematical expectation in both sides of inequality takes different values and, hence, a correcting factor F has been added to the inequality in order to maintain the same value in both sides as well as to obtain a good approximation on the ergodic capacity analysis of MIMO FSO systems [38, 53]. The correcting factor F can be derived from Eq. (13) as follows

$$F = \frac{\mathbb{E}\left[\sum_{k=1}^{M}\sum_{l=1}^{N} I_{kl}\right]^{MN}}{(MN)^{MN} \cdot \mathbb{E}\left[\sqrt[MN]{\prod_{k=1}^{M}\prod_{l=1}^{N} I_{kl}}\right]^{MN}}. \tag{14}$$

In addition, this correcting factor F only depends on channel parameters and can be seen in more detail in appendix A. Now, substituting Eq. (13) into Eq. (12) and, after, performing some algebraic manipulations, the ergodic capacity for a MIMO FSO system can accurately be approximated as follows

$$C_{\mathrm{MIMO}} \simeq \frac{B}{\ln(4)} \underbrace{\int_0^{\infty} \cdots \int_0^{\infty}}_{\text{MN-fold}} \ln\left(1 + 4\gamma_0 F^{\frac{2}{MN}}\left(\prod_{k=1}^{M}\prod_{l=1}^{N} i_{kl}\right)^{\frac{2}{MN}}\right) \prod_{k=1}^{M}\prod_{l=1}^{N} f_{I_{kl}}(i_{kl})di_{kl}. \tag{15}$$

At this time, to the authors' best knowledge, the integral in Eq. (15) is highly complex to find an exact solution even might not be expressed as a closed-form expression. For this reason, an asymptotic analysis is carried out in this paper and, hence, simple closed-form expressions in the analysis of the ergodic capacity of MIMO FSO systems are derived. An asymptotic expression at high SNR can be readily and accurately lower-bounded due to the fact that $\ln(1+z) \approx \ln(z)$ when $z \to \infty$ as follows

$$C_{\mathrm{MIMO}} \doteq \frac{B}{\ln(4)} \underbrace{\int_0^{\infty} \cdots \int_0^{\infty}}_{\text{MN-fold}} \ln\left(4\gamma_0 F^{\frac{2}{MN}}\left(\prod_{k=1}^{M}\prod_{l=1}^{N} i_{kl}\right)^{\frac{2}{MN}}\right) \prod_{k=1}^{M}\prod_{l=1}^{N} f_{I_{kl}}(i_{kl})di_{kl}. \tag{16}$$

#255615 Received 11 Dec 2015; revised 22 Jan 2016; accepted 28 Jan 2016; published 10 Feb 2016
© 2016 OSA

By applying the following identity: $\ln(a\cdot b)=\ln(a)+\ln(b)$ in Eq. (16) as

$$\ln\left(4\gamma_0 F^{\frac{2}{MN}}\left(\prod_{k=1}^{M}\prod_{l=1}^{N} i_{kl}\right)^{\frac{2}{MN}}\right)=\ln(4\gamma_0)+\frac{2}{MN}\ln(F)+\frac{2}{MN}\sum_{k=1}^{M}\sum_{l=1}^{N}\ln(i_{kl}), \tag{17}$$

we can rewrite the integral in Eq. (16) as follows

$$C_{\text{MIMO}}\doteq\frac{B\ln(4\gamma_0)}{\ln(4)}+\frac{B\ln(F)}{MN\ln(2)}+\frac{B}{MN\ln(2)}\sum_{k=1}^{M}\sum_{l=1}^{N}\underbrace{\int_0^{\infty}\ln(i_{kl})f_{I_{kl}}(i_{kl})di_{kl}}_{INT}. \tag{18}$$

Another way of obtaining the ergodic capacity of FSO communication systems at high SNR is via utilizing moments method, presented for the first time in [54, Eqs. (8) and (9)], as in [6, 55, 56]. Knowing that the atmospheric turbulence and pointing errors are statistically independent, the integral INT in Eq. (18) can be rewritten as follows

$$\begin{aligned}INT&=\int_0^{\infty}\ln(i_{kl})f_{I_{kl}}(i_{kl})di_{kl}=\int_0^{\infty}\int_0^{A_{0_{kl}}}\ln(L_{kl}\cdot i_{kl}^a\cdot i_{kl}^p)f_{I_{kl}^a}(i_{kl}^a)f_{I_{kl}^p}(i_{kl}^p)di_{kl}^a di_{kl}^p\\&=\ln(L_{kl})+\underbrace{\int_0^{\infty}\ln(i_{kl}^a)f_{I_{kl}^a}(i_{kl}^a)di_{kl}^a}_{INT_1}+\underbrace{\int_0^{A_{0_{kl}}}\ln(i_{kl}^p)f_{I_{kl}^p}(i_{kl}^p)di_{kl}^p}_{INT_2}=\ln(L_{kl})+INT_1+INT_2.\end{aligned} \tag{19}$$

Firstly, we derive INT_2 in appendix B as follows

$$INT_2=\int_0^{A_{0_{kl}}}\ln(i_{kl}^p)f_{I_{kl}^p}(i_{kl}^p)di_{kl}^p=\ln(A_{0_{kl}})-\frac{1}{\varphi_{kl}^2}-\frac{s_{kl}^2}{2\sigma_{s_{kl}}^2\varphi_{kl}^2}. \tag{20}$$

Next, we solve the integral INT_1 in Eq. (18) for each considered turbulence scenario in this ergodic capacity analysis of MIMO FSO communication systems.

4.1. Log-normal (LN) atmospheric turbulence scenario

By making a change of variable $t=\ln(x)$, it can easily be deduced that the result of integral INT_1 for LN atmospheric turbulence is $INT_1^{\text{LN}}=-\sigma_{R_{kl}}^2/2$. Hence, the asymptotic closed-form solution for the ergodic capacity of MIMO FSO systems over LN fading channels with nonzero boresight pointing errors can be expressed as

$$\begin{aligned}C_{\text{MIMO}}^{\text{LN}}&\doteq\frac{B\ln(4\gamma_0)}{\ln(4)}+\frac{B\ln(F)}{MN\ln(2)}\\&+\frac{B}{MN\ln(2)}\sum_{k=1}^{M}\sum_{l=1}^{N}\ln(L_{kl})-\frac{\sigma_{R_{kl}}^2}{2}+\ln(A_{0_{kl}})-\frac{1}{\varphi_{kl}^2}-\frac{s_{kl}^2}{2\sigma_{s_{kl}}^2\varphi_{kl}^2}.\end{aligned} \tag{21}$$

4.2. Gamma-Gamma (GG) atmospheric turbulence scenario

To evaluate the integral INT_1 for GG atmospheric turbulence, i.e. INT_1^{GG}, we can use that the $K_\nu(\cdot)$ function is related to $J_\nu(\cdot)$ function by using [57, eqn. (03.04.27.0001.01)] and, then, we can also use that the $J_\nu(\cdot)$ function is related to $I_\nu(\cdot)$ by using [57, eqn. (03.02.27.0001.01)]. Next, using [43, eqn. (6.771)] and, then, performing some algebraic manipulations, we can express INT_1^{GG} as follows

$$INT_1^{\text{GG}}=\ln\left(\frac{1}{\alpha_{kl}\beta_{kl}}\right)+\psi(\alpha_{kl})+\psi(\beta_{kl}), \tag{22}$$

#255615 Received 11 Dec 2015; revised 22 Jan 2016; accepted 28 Jan 2016; published 10 Feb 2016
© 2016 OSA

where $\psi(\cdot)$ is the psi (digamma) function [43, eqn. (8.360.1)]. Hence, the asymptotic closed-form solution for the ergodic capacity of MIMO FSO systems over GG fading channels with nonzero boresight pointing errors can be expressed as

$$C_{\text{MIMO}}^{\text{GG}} \doteq \frac{B\ln(4\gamma_0)}{\ln(4)} + \frac{B\ln(F)}{MN\ln(2)} + \frac{B}{MN\ln(2)} \sum_{k=1}^{M}\sum_{l=1}^{N} \ln\left(\frac{L_{kl}}{\alpha_{kl}\beta_{kl}}\right) + \psi(\alpha_{kl}) + \psi(\beta_{kl}) + \ln(A_{0_{kl}}) - \frac{1}{\varphi_{kl}^2} - \frac{s_{kl}^2}{2\sigma_{s_{kl}}^2\varphi_{kl}^2}. \tag{23}$$

4.3. Exponentiated Weibull (EW) atmospheric turbulence scenario

In order to compute the integral INT_1 for EW atmospheric turbulence, i.e. INT_1^{EW}, we write the corresponding integral as follows

$$INT_1^{EW} = \frac{ab}{c}\int_0^{\infty} \ln(i)\left(\frac{i}{c}\right)^{b-1} \exp\left(-\left(\frac{i}{c}\right)^{b}\right)\left\{1-\exp\left(-\left(\frac{i}{c}\right)^{b}\right)\right\}^{a-1} di. \tag{24}$$

Using the corresponding series expansion of $(1+e^x)^{\alpha}$ as follows

$$(1+e^x)^{\alpha} = \sum_{k=1}^{\infty} \frac{\Gamma(\alpha+1)e^{xk}}{k!\Gamma(\alpha-k+1)}. \tag{25}$$

The integral in Eq. (24) can be rewritten as

$$INT_1^{EW} = \frac{b\Gamma(a+1)}{c^b}\sum_{k=0}^{\infty}\frac{(-1)^k}{k!\Gamma(a-k)}\int_0^{\infty}\ln(i)i^{b-1}\exp\left(-(k+1)\left(\frac{i}{c}\right)^{b}\right) di. \tag{26}$$

To evaluate the integral in Eq. (26), we can make a change of variable $x = i^b$ and the fact that $\int_0^{\infty} x^{\nu-1}e^{-\mu x}\ln(x)dx = \frac{\Gamma(\nu)}{\mu^{\nu}}[\psi(\nu)-\ln(\mu)]$ [43, eqn. (4.352.1)], obtaining the corresponding closed-form asymptotic solution for the ergodic capacity of MIMO FSO systems over EW fading channels with nonzero boresight pointing errors that can be expressed as

$$C_{\text{MIMO}}^{\text{EW}} \doteq \frac{B\ln(4\gamma_0)}{\ln(4)} + \frac{B\ln(F)}{MN\ln(2)} + \frac{B}{MN\ln(2)} \times \sum_{k=1}^{M}\sum_{l=1}^{N} \ln(L_{kl}) + g(a_{kl},b_{kl},c_{kl}) + \ln(A_{0_{kl}}) - \frac{1}{\varphi_{kl}^2} - \frac{s_{kl}^2}{2\sigma_{s_{kl}}^2\varphi_{kl}^2}, \tag{27}$$

where $g(a_{kl},b_{kl},c_{kl})$ is given by

$$g(a_{kl},b_{kl},c_{kl}) = \frac{\Gamma(a_{kl}+1)}{b_{kl}}\sum_{i=0}^{\infty}\frac{(-1)^i\left(\psi(1)-\ln\left((i+1)\left(\frac{1}{c_{kl}}\right)^{b_{kl}}\right)\right)}{\Gamma(i+2)\Gamma(a_{kl}-i)}, \tag{28}$$

wherein $-\psi(1)$ is the Euler's constant. Note that Eq. (28) can easily be computed as the series converges fast, and usually as much as 20 terms or less are sufficient for the series to converge.

5. Numerical results and discussions

For the sake of simplicity, the numerical results are evaluated for independent and identically distributed (i.i.d.) atmospheric turbulence channels with pointing errors but considering nonzero inherent boresight displacements and zero additional boresight error, i.e.

#255615 Received 11 Dec 2015; revised 22 Jan 2016; accepted 28 Jan 2016; published 10 Feb 2016
© 2016 OSA

$(\Delta x, \Delta y) = (0,0)$. In other words, when the alignment point $p_c = p'_c$. The impact of nonzero additional boresight error is studied in the subsection 5.2. As commented in Section 2, due to the fact that the distance between transmit lasers and receiver is several orders of magnitude the spacing between transmitters, the MIMO FSO channel can be considered as i.i.d, obtaining the similar results as in i.n.i.d. fading channels, as demonstrated in [38].

As an illustration of the obtained asymptotic ergodic capacity expressions, numerical results under LN, GG and EW fading channels are depicted in Figs. 3(a), 3(b) and 4, respectively. Without loss of generality, we consider some scenarios as case study of MISO, SIMO and MIMO FSO communication systems when all transmit lasers are aligned with the centroid of the geometric arrangement at the receiver, as commented in section 2. In this way, different values of M and N are taken into account in order to analyze how the effect of nonzero inherent boresight pointing errors impacts on the ergodic capacity of SIMO and MIMO FSO systems when point-like receiver apertures are considered for LN and GG atmospheric tubulence, i.e., $D \leq \rho_0$ and, when aperture averaging takes place for EW, i.e., $D \geq \rho_0$. Different weather conditions are adopted in this study: haze visibility of 4 km with $C_n^2 = 1.7 \times 10^{-14}\ m^{-2/3}$ and $C_n^2 = 2 \times 10^{-14}\ m^{-2/3}$ and clear visibility of 16 km with $C_n^2 = 8 \times 10^{-14}\ m^{-2/3}$, corresponding to moderate and strong turbulence conditions, respectively. A value of wavelength of $\lambda = 1550$ nm is chosen. Pointing errors are present here assuming values of normalized beam width and normalized jitter of $(\omega_z/r, \sigma_s/r) = (5,1)$ and $(\omega_z/r, \sigma_s/r) = (10,2)$. A source-destination link distance of $d_{SD} = 1$ km and a value of normalized spacing between receiver apertures of $d'/r = 8$ as well as a source-destination link distance of $d_{SD} = 2$ km and a value of normalized spacing between receiver apertures of $d'/r = 10$ are considered for LN and GG atmospheric turbulence, respectively. Here, parameters α and β are calculated from Eq. (4) for GG atmospheric turbulence. Analogously, a source-destination link distance of $d_{SD} = 3$ km as well as values of spacing among receiver apertures of $d' = 15$ mm and $d' = 25$ mm are considered when the radius r of the receive aperture corresponding to the SISO FSO system is set to 7.5 mm and 10 mm respectively, for EW atmospheric turbulence. The corresponding radius of SIMO and MIMO FSO systems is equal to $r = r_{SISO}/\sqrt{N}$. Here, parameters a, b and c are calculated from Eq. (6) for EW atmospheric turbulence. Additionally, we also include the performance analysis for the direct path link in order to establish the baseline performance, i.e., when the parameter M and N are set to 1 in Eq. (18) regardless of the considered statistical model of atmospheric turbulence. To confirm the accuracy and usefulness of the derived bounds, Monte Carlo simulation results, where the MIMO FSO channel is modeled by using the statistical model given by $Y = \eta XI + Z$ are furthermore included by using solid line generating the corresponding variates from the exact combined PDF. It is noteworthy to mention that the obtained results provide an excellent match between the analytical and the respective Monte Carlo simulation results, which are obtained from Eq. (12), and, hence, verifying the high accuracy of the proposed approximation. In addition, these figures also show the high accuracy of the asymptotic results based on the logarithm approximation given in Eq. (18) at high SNR. Taking into account the logarithm approximation, a good agreement between simulation results and asymptotic results is achieved when the received electrical SNR is at least an order of magnitude higher than 1, i.e., higher than 10. In this case, it is easily deduced that the received electrical signal in absence of turbulence, $\gamma_0[dB]$, must be higher than $10\log_{10}(10M^2N^2/4\left(MN\mathbb{E}[I^2] + MN(MN-1)\mathbb{E}[I]^2\right))$ when i.i.d. fading channels are assumed. As can be seen in Fig. 3, a MISO FSO system present a much better performance than SIMO and MIMO FSO systems in terms of the ergodic capacity, keeping the product $M \cdot N = 4$ and not considering the additional boresight error. It must be noted that both SIMO and MIMO present a nonzero inherent boresight displacement, which depends on the distance between the alignment point and each receive aperture and, hence, the obtained performance is significantly

#255615 Received 11 Dec 2015; revised 22 Jan 2016; accepted 28 Jan 2016; published 10 Feb 2016
© 2016 OSA

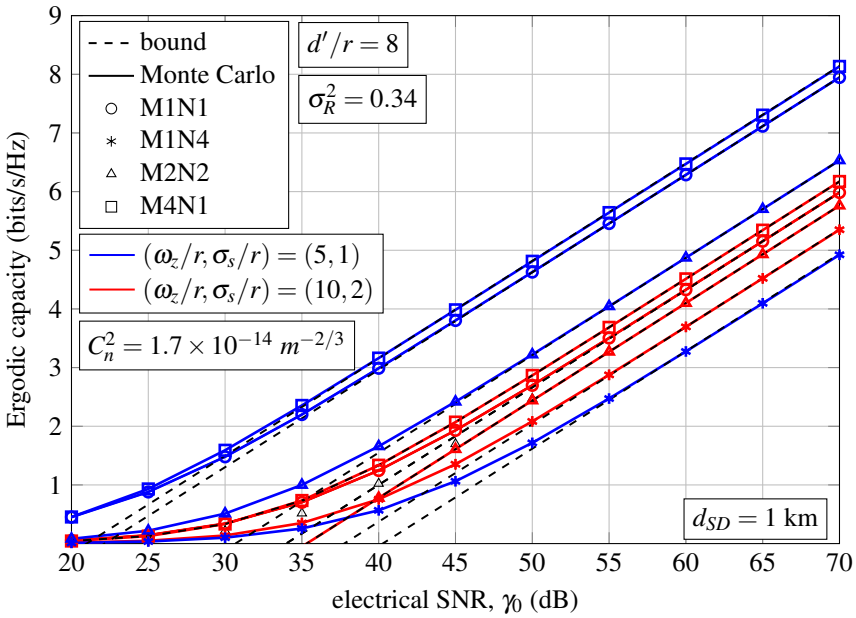

(a) log-normal

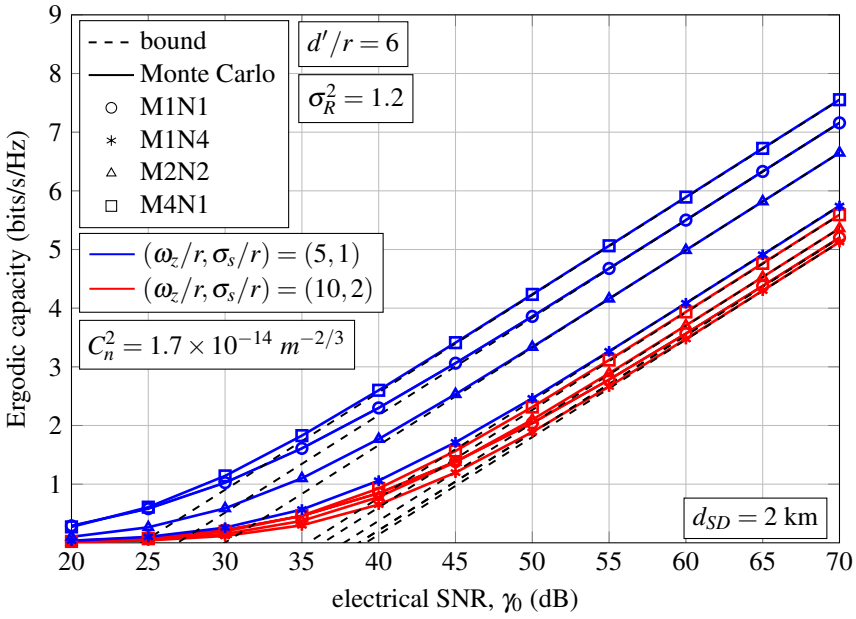

(b) gamma-gamma

Fig. 3. Asymptotic ergodic capacity of MIMO FSO systems when (a) LN and (b) GG atmospheric turbulence models are assumed for different values of normalized beam width and normalized jitter of $(\omega_z/r, \sigma_s/r) = \{(5,1),(10,2)\}$ as well as different values of normalized spacing among receive apertures of $d'/r = \{6,8\}$.

#255615 Received 11 Dec 2015; revised 22 Jan 2016; accepted 28 Jan 2016; published 10 Feb 2016
© 2016 OSA

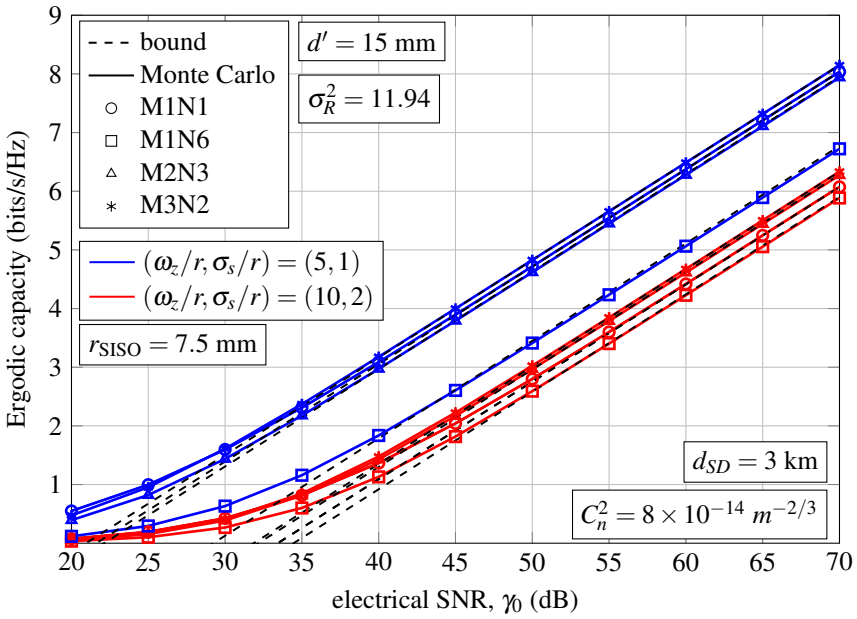

(a) exponentiated Weibull

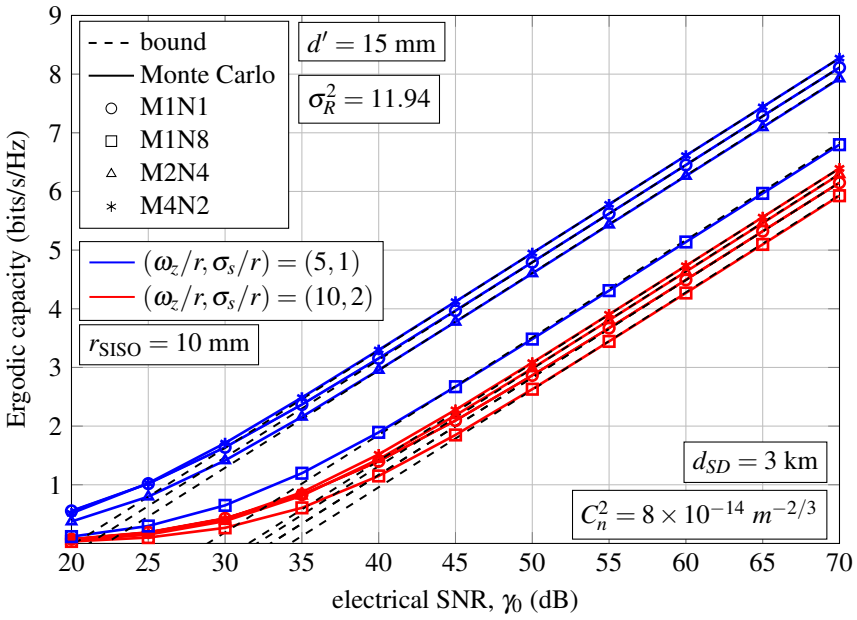

(b) exponentiated Weibull

Fig. 4. Asymptotic ergodic capacity of MIMO FSO systems over EW atmospheric turbulence for different values of normalized beam width and normalized jitter of $(\omega_z/r, \sigma_s/r) = \{(5,1),(10,2)\}$.

#255615 Received 11 Dec 2015; revised 22 Jan 2016; accepted 28 Jan 2016; published 10 Feb 2016
© 2016 OSA

reduced. Therefore, a FSO system with multiple receive apertures can improve the capacity of the direct path link when the spacing among receive apertures is not too big in order to reduce the effect of nonzero inherent boresight. Alternatively, the obtained performance corresponding to SISO and MISO FSO systems depend on the additional boresight error, which will be studied at the end of this section. These conclusion are totally valid for EW atmospheric turbulence in Fig. 4, when the aperture averaging takes place and the product $M \cdot N$ is equal to 6. Alternatively, the effect of beam width and jitter is also discussed. As expected, as the normalized beam width increases, i.e. from $\omega_z/r = 5$ to $\omega_z/r = 10$, the performance also decreases. As a result, an increase in the normalized beam width not only leads to a greater deterioration in the performance, but also to a reduction of the effect of inherent boresight displacement.

5.1. Comparison among different geometric arrangements at the receiver

Now, we examine different geometric arrangements for the receiver in order to make a fair comparison between the method proposed in section 2 and other more typical geometric arrangements, as shown in Fig. 5. In this way, we compare three different configurations when the value of M is equal to 1 and the value of N is equal to 8, i.e a SIMO FSO system with eight receive apertures. In Fig. 5(a), an heptagon is depicted where one receive aperture is located at the center and the rest of receive apertures are equally spaced around a circle (d'), whose radius is equal to $d'/2\sin(\pi/7)$. In Fig. 5(b), a rectangle is depicted wherein all receive apertures are separated by a distance equals d'. In both geometric arrangements, their corresponding centroid is the alignment point. From Eq. (20), we can see that the effect of nonzero boresight appears as a sum of squares ($\sum_{k=1}^{M}\sum_{l=1}^{N} s_{kl}^2$) and, hence, the methodology based on the juxtaposition of triangle equilaterals is able to minimize the sum of square, $\sum_{k=1}^{M}\sum_{l=1}^{N} s_{kl}^2$, respect to the receiver configurations depicted in Fig. 5. It is easily deduced that the sum of square corresponding to the formed figure in Fig. 2(g) is equal to $8.68{d'}^2$ while the formed figure in Figs. 5(a) and 5(b) is equal to $9.29{d'}^2$ and $12{d'}^2$, respectively. This conclusion is corroborated in Fig. 6. However, it should be noted that this methodology does not provide the optimal performance due to the fact that finding the best method can be time-consuming and is often technically difficult to perform. As can be seen in Fig. 6, a source-destination link distance of $d_{SD} = 4$ km as well

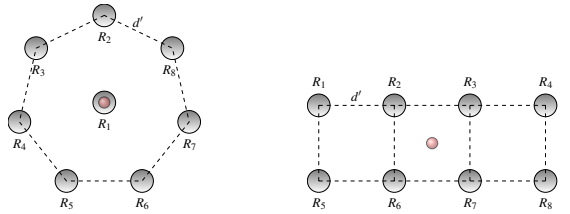

(a) Heptagon (b) Rectangle

Fig. 5. Receive apertures.

as values of spacing among receiver apertures of $d' = 12$ mm and $d' = 24$ mm are considered when the radius r of receive aperture corresponding to the SISO FSO system is set to 15 mm for EW atmospheric turbulence. As commented before, depending on the distance among receive apertures, the effect of nonzero inherent boresight displacement can be more severe. It should be highlighted that the proposed geometric arrangement for the receiver is able to achieve a better performance than other more typical geometric arrangements such as Figs. 5(a) and 5(b).

#255615 Received 11 Dec 2015; revised 22 Jan 2016; accepted 28 Jan 2016; published 10 Feb 2016
© 2016 OSA

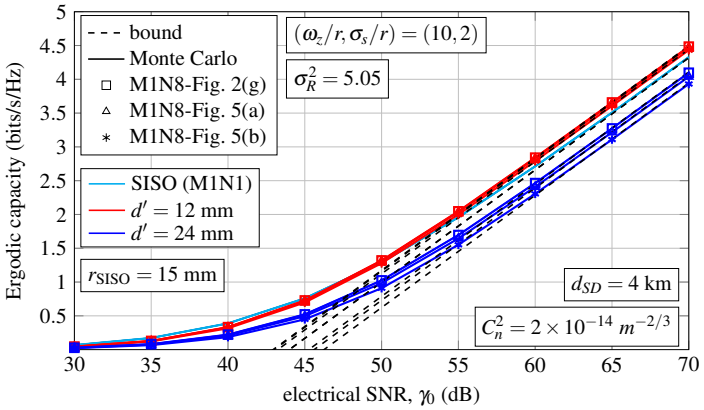

Fig. 6. Comparison among different geometric arrangements for the receiver over EW atmospheric turbulence when different values of spacing among receive apertures of $d' = \{12 \text{ mm}, 24 \text{ mm}\}$.

5.2. *Impact of nonzero additional boresight error*

The impact of nonzero additional boresight error (s_{AB}, defined in section 2) on the ergodic capacity of MIMO FSO systems is also analyzed, which only depends on the number of receive apertures and pointing error parameters such as beam width, boresight error and alignment point. From the asymptotic ergodic capacity analysis carried out in section 4, we can obtain the disadvantage in decibels between considering and not considering nonzero additional boresight error. To do this, the ergodic asymptotic capacity analysis can be extended in order to obtain a point where the asymptotic ergodic capacity intersects with the γ_0-axis at high SNR ($C/B = 0$ bits/s/Hz), as demonstrated in [38, 53, 56]. This point can be understood as a SNR threshold, i.e. $\gamma_{\text{MIMO}}^{th}$, in which the ergodic capacity of MIMO FSO systems is significantly increased. Hence, the corresponding expression of $\gamma_{\text{MIMO}}^{th}$ in terms of the channel parameters can be derived as

$$\gamma_{\text{MIMO}}^{th}[dB] = \frac{-20}{\ln(10)}\left(\frac{\ln(F)}{MN} + \ln(2) + \frac{1}{MN}\sum_{k=1}^{M}\sum_{l=1}^{N}\ln(L_{kl}) + INT_1 + \ln(A_{0_{kl}}) - \frac{1}{\varphi_{kl}^2} - \frac{s_{kl}^2}{2\sigma_{s_{kl}}^2\varphi_{kl}^2}\right), \tag{29}$$

where the value of INT_1 depends on the selected atmospheric turbulence model, i.e., LN (Eq. (21)), GG (Eq. (23)) and EW (Eq. (27)). Next, it can be easily deduced from this asymptotic analysis at high SNR that the shift of the ergodic capacity versus SNR is more relevant than the slope of the curve in SNR compared to other performance metrics such as BER and outage probability. This shift can be interpreted as an improvement on ergodic capacity in order to maintain the same performance in terms of capacity with less SNR. In this way, taking into account this latter, it can be deduced that this disadvantage, $D_{AB}[dB]$, can be written as

$$\begin{aligned} D_{AB}[dB] &= \gamma_{th}^{NZAB}[dB] - \gamma_{th}^{NZIB}[dB] \\ &= \frac{20\ln\left(F^{NZIB}/F^{NZAB}\right)}{MN\ln(10)} + \frac{10}{MN\ln(10)\sigma_s^2\varphi^2}\sum_{k=1}^{M}\sum_{l=1}^{N}s_{AB}^2 - 2\left(\Delta x \cdot x_{kl} + \Delta y \cdot y_{kl}\right), \end{aligned} \tag{30}$$

where F^{NZIB} represents the correcting factor taking into account the inherent boresight displacement and F^{NZAB} represents both the inherent boresight displacement and the additional

#255615 Received 11 Dec 2015; revised 22 Jan 2016; accepted 28 Jan 2016; published 10 Feb 2016
© 2016 OSA

boresight error. It should be noted that the above expression does not depend on the atmospheric turbulence. This expression not only depends on the pointing errors parameters but also on the geometric arrangements of the receive apertures at the receiver. In this way, this disad-

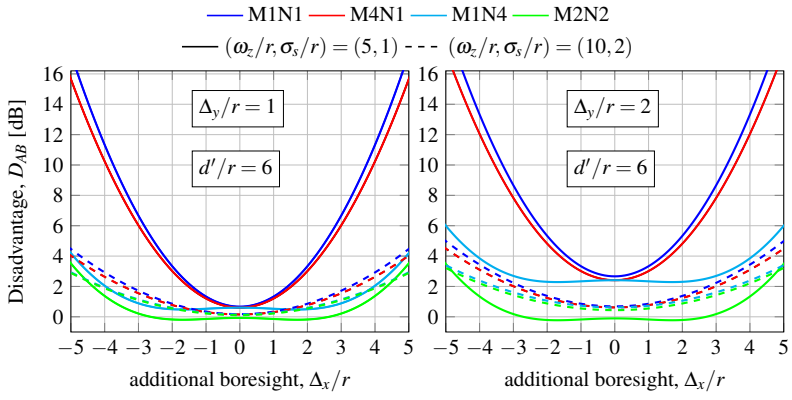

(a) additional boresight error

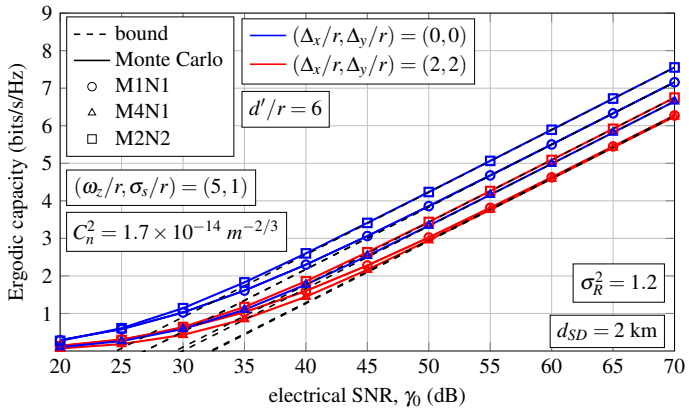

(b) gamma-gamma

Fig. 7. (a) Disadvantage as a function of the horizontal displacement of the normalized additional boresight error when different values of normalized beam width and normalized jitter of $(\omega_z/r, \sigma_s/r) = \{(5,1),(10,2)\}$ are considered and, (b) performance over gamma-gamma atmospheric turbulence.

vantage is depicted in Fig. 7(a) as a function of the horizontal displacement of the normalized additional boresight error, Δ_x/r, for different values of vertical displacement of the normalized boresight error of $\Delta_y/r = \{1,2\}$. Values of normalized beam width and normalized jitter of $(\omega_z/r, \sigma_s/r) = \{(5,1),(10,2)\}$ as well as different values of M and N are also considered. As expected, the effect of nonzero additional boresight error can dramatically reduce the ergodic capacity corresponding to systems with values of $N = 1$ (number of receiver apertures), i.e., SISO and MISO FSO systems. In addition to this, the performance has not been so affected by the presence of a nonzero additional boresight error when the parameter $N > 1$, i.e. MIMO and SIMO FSO systems. This latter is owing to the robustness provided by the centroid as a alignment point. Finally, Fig. 7(b) is added to this study in order to contrast some obtained values of the disadvantage, $D_{AB}[dB]$, considering the same scenario corresponding to Fig. 3(b). It can be

#255615 Received 11 Dec 2015; revised 22 Jan 2016; accepted 28 Jan 2016; published 10 Feb 2016
© 2016 OSA

seen in this figure that values of disadvantages of 5.32 dB, 4.81 dB and 2.3 dB corresponding to SISO, MISO and MIMO FSO systems, respectively, are obtained for values of normalized beam width and normalized jitter of $(\omega_z/r, \sigma_s/r) = (5,1)$.

6. Conclusions

The impact of nonzero boresight pointing errors on the ergodic capacity of MIMO FSO systems with EGC reception under different turbulence models such as LN, GG as well as EW has been studied. A new boresight error has been taken into consideration in this paper, which is always present in receive-diversity FSO systems. Novel closed-form asymptotic expressions at high SNR for the ergodic capacity of MIMO FSO systems has been derived when different geometric arrangements of the receive apertures are considered. On the one hand, it is concluded that the use of SIMO and MIMO techniques can significantly increase the ergodic capacity respect to the direct path link when the inherent boresight displacement takes small values, i.e. when the spacing among receive apertures is not too big. On the other hand, a MISO FSO system is able to achieve a higher performance when the additional boresight error is not considered. At the same time, the effect of nonzero additional boresight errors has also been evaluated for MIMO FSO communication systems. It is noteworthy to mention that the dominant effects in the ergodic capacity of MIMO FSO channels are both atmospheric turbulence and nonzero pointing errors. In addition to this, a new methodology has been proposed in order to generate different receiver configurations from the juxtaposition of equilateral triangles, which guarantee a notable reduction of the effect of the inherent boresight displacement against other geometric arrangements at the receiver. Finally, from the relevant results derived here, researching the impact of nonzero boresight pointing errors on the ergodic capacity of MIMO FSO systems over $\mathscr{M}$-distributed atmospheric turbulence [58] and/or Double GG generalized fading channels [59, 60] as well as considering other pointing error models are interesting topics for future research in order to complement the analysis in this paper.

Appendix A

As commented before, we can express the correcting factor, F, as follows

$$F = \frac{\mathbb{E}\left[\sum_{k=1}^{M}\sum_{l=1}^{N} I_{kl}\right]^{MN}}{(MN)^{MN}\cdot\mathbb{E}\left[\sqrt[MN]{\prod_{k=1}^{M}\prod_{l=1}^{N} I_{kl}}\right]^{MN}} = \frac{\left(\sum_{k=1}^{M}\sum_{l=1}^{N}\mathbb{E}\left[I_{kl}\right]\right)^{MN}}{(MN)^{MN}\cdot\left(\prod_{k=1}^{M}\prod_{l=1}^{N}\mathbb{E}\left[\sqrt[MN]{I_{kl}}\right]\right)^{MN}}. \quad (31)$$

In order to compute the correcting factor F given in Eq. (31), we have to obtain the nth moment of I, i.e., $I = L\cdot I^a\cdot I^p$ knowing that I^a and I^p and statistically independent as follows

$$\mathbb{E}[I^n] = \mathbb{E}[(L\cdot I^a\cdot I^p)^n] = L^n\cdot\mathbb{E}[(I^a)^n]\cdot\mathbb{E}[(I^p)^n] = L^n\cdot\int_0^{\infty} x^n f_{I^a}(x)dx\cdot\int_0^{A_0} y^n f_{I^p}^{NZB}(y)dy. \quad (32)$$

Firstly, we derive the nth moment corresponding to the nonzero boresight pointing error, which was derived in [3, appendix B] as follows

$$\mathbb{E}\left[\left(I_p^{NZB}\right)^n\right] = \frac{A_0\varphi^2}{n+\varphi^2}\exp\left(-\frac{ns^2}{(n+\varphi^2)2\sigma_s^2}\right). \quad (33)$$

Secondly, we derive the nth moment corresponding to LN turbulence scenario as

$$\mathbb{E}\left[\left(I_a^{LN}\right)^n\right] = \exp\left(\frac{n\sigma_R^2}{2}(n-1)\right). \quad (34)$$

#255615 Received 11 Dec 2015; revised 22 Jan 2016; accepted 28 Jan 2016; published 10 Feb 2016
© 2016 OSA

Next, the nth moment corresponding to GG turbulence scenario can be written as

$$\mathbb{E}\left[\left(I_a^{GG}\right)^n\right] = \left(\frac{1}{\alpha\beta}\right)^n \frac{\Gamma(n+\alpha)\Gamma(n+\beta)}{\Gamma(\alpha)\Gamma(\beta)}. \tag{35}$$

The nth moment corresponding to the EW turbulence scenario was derived for any a (both real and integer) in [61] as

$$\mathbb{E}\left[\left(I_a^{EW}\right)^n\right] = ac^n\Gamma\left(1+\frac{n}{b}\right) g_n(a,b). \tag{36}$$

As in Eq. (28), the summation in Eq. (36) can also easily be computed as the series converges fast, and usually as much as 20 terms or less are sufficient for the series to converge. Finally, the correcting factor F is derived substituting Eq. (33) into Eq. (31) and, substituting Eq. (34), Eq. (35) or Eq. (36) into Eq. (31) depending on the considered atmospheric turbulence scenario.

Appendix B

Substituting Eq. (8) into Eq. (20), we obtain

$$\frac{\varphi^2 \exp\left(-\frac{s^2}{2\sigma_s^2}\right)}{A^{\varphi^2}} \int_0^{A_0} \ln(x) x^{\varphi^2-1} I_0\left(\frac{s}{\sigma_s}\sqrt{-2\varphi^2 \ln\left(\frac{x}{A_0}\right)}\right) dx. \tag{37}$$

Using the Maclaurin series expansion of $I_0(\cdot)$ [43, eqn. (8.445)], we have

$$\frac{\varphi^2 \exp\left(-\frac{s^2}{2\sigma_s^2}\right)}{A^{\varphi^2}} \int_0^{A_0} \ln(x) x^{\varphi^2-1} \sum_{k=0}^{\infty} \frac{(-2\varphi^2)^k \left(\frac{s}{2\sigma_s}\right)^{2k}}{k!\Gamma(k+1)} \ln(x/A_0)^k dx. \tag{38}$$

Since each term of the series is non-negative and the infinite series uniformly converges to $I_0\left(\frac{s}{\sigma_s}\sqrt{-2\varphi^2 \ln\left(\frac{x}{A_0}\right)}\right)$, we can swap the integral and infinite summation and write Eq. (37) as follows

$$\begin{aligned} &\frac{\varphi^2 \exp\left(-\frac{s^2}{2\sigma_s^2}\right)}{A^{\varphi^2}} \sum_{k=0}^{\infty} \frac{(-2\varphi^2)^k \left(\frac{s}{2\sigma_s}\right)^{2k}}{k!\Gamma(k+1)} \int_0^{A_0} \ln(x) x^{\varphi^2-1} \ln(x/A_0)^k dx \\ &= \varphi^2 \exp\left(-\frac{s^2}{2\sigma_s^2}\right) \sum_{k=0}^{\infty} \frac{(-2\varphi^2)^k \left(\frac{s}{2\sigma_s}\right)^{2k}}{k!\Gamma(k+1)} \int_0^1 \ln(xA_0) x^{\varphi^2-1} \ln(x)^k dx. \end{aligned} \tag{39}$$

The integral in Eq. (39) can be expressed as a sum of two integrals as follows

$$\int_0^1 \ln(xA_0) x^{\varphi^2-1} \ln(x)^k dx = \ln(A_0) \int_0^1 x^{\varphi^2-1} \ln(x)^k dx + \int_0^1 x^{\varphi^2-1} \ln(x)^{k+1} dx. \tag{40}$$

Both integrals in Eq. (40) can be solved with the help of [43, eqn. (4.294.10)] and making a change of variable $t = x-1$. Then, performing some straightforward algebraic manipulations,

#255615 Received 11 Dec 2015; revised 22 Jan 2016; accepted 28 Jan 2016; published 10 Feb 2016
© 2016 OSA

the expression in Eq. (39) can be written as

$$\begin{aligned}
&\exp\left(-\frac{s^2}{2\sigma_s^2}\right)\sum_{k=0}^{\infty}\frac{\left(\frac{s^2}{2\sigma_s^2}\right)^k}{k!}\left(\frac{\ln(A_0)-1-k}{\varphi^2}\right)\\
&=\exp\left(-\frac{s^2}{2\sigma_s^2}\right)\left\{\left(\ln(A_0)-\frac{1}{\varphi^2}\right)\sum_{k=0}^{\infty}\frac{\left(\frac{s^2}{2\sigma_s^2}\right)^k}{k!}-\sum_{k=0}^{\infty}\frac{k\left(\frac{s^2}{2\sigma_s^2}\right)^k}{\varphi^2 k!}\right\}\\
&=\exp\left(-\frac{s^2}{2\sigma_s^2}\right)\left\{\left(\ln(A_0)-\frac{1}{\varphi^2}\right)\sum_{k=0}^{\infty}\frac{\left(\frac{s^2}{2\sigma_s^2}\right)^k}{k!}-\frac{s^2}{2\varphi^2\sigma_s^2}\sum_{k=1}^{\infty}\frac{\left(\frac{s^2}{2\sigma_s^2}\right)^{k-1}}{(k-1)!}\right\}.
\end{aligned} \tag{41}$$

Knowing that $e^x=\sum_{k=0}^{\infty}\frac{x^k}{k!}$ [43, eqn. (1.211.1)], the impact of nonzero boresight pointing error on the ergodic capacity of MIMO FSO systems can be written as

$$\begin{aligned}
&\exp\left(-\frac{s^2}{2\sigma_s^2}\right)\left\{\left(\ln(A_0)-\frac{1}{\varphi^2}\right)\exp\left(\frac{s^2}{2\sigma_s^2}\right)-\frac{s^2}{2\varphi^2\sigma_s^2}\exp\left(\frac{s^2}{2\sigma_s^2}\right)\right\}\\
&=\ln(A_0)-\frac{1}{\varphi^2}-\frac{s^2}{2\sigma_s^2\varphi^2}.
\end{aligned} \tag{42}$$

Acknowledgment

The authors would like to thank the anonymous reviewers for their useful comments that helped to improve the presentation of this manuscript. The authors are grateful for financial support from the Junta de Andalucía (research group Communications Engineering (TIC-0102)).

#255615 Received 11 Dec 2015; revised 22 Jan 2016; accepted 28 Jan 2016; published 10 Feb 2016
© 2016 OSA